Impact of Flame-Flame Interaction in Identical Two Non-premixed Microflames

Taro Hirasawa [a*], Kunihiro Gotanda [a], Hiroki Masuda [b], Yuji Nakamura [b]

[a] Department of Mechanical Engineering, Chubu University
Kasugai, Aichi, Japan
[b] Division of Mechanical and Space Engineering, Hokkaido University
Sapporo, Hokkaido, Japan

1 Introduction

Micro-scale flame has been studied mainly for the application of micro combustor for recent years [e.g., 1]. Through those studies, non-premixed microflame is found to be distinctive advantages for its emission; it produces little NO_x and hardly forms soot *without* any special treatment (e.g., premixing, dilution etc.) [e.g., 2]. In general, non-premixed flame is easy and safe to use due to high stability, that is, no flush back and being hard to be lifted. Then, non-premixed microflame gains attractiveness for its application use. Microflame has also advantage in high density of heat release value i.e. heat release per unit volume because volume for combustion is relatively small. Even though microflame has attractive feature, its heat release value is too small to meet existing ordinary demands. This disadvantage, however, is easily solved by arranging multiple microflames side-by-side, which is what we call "microflame-array (MFA) [2]". In addition to heritage from microflame, the microflame array has advantage in working as uniform plane heating device [3]. We have successfully made a miniature MFA burner whose thickness is 6 mm and burner pitch is less than 4 mm to achieve combustion load more than 65W/cm^2.

Upon the development of MFA burner, it is found that the flame-flame interaction has a significant impact on its performance. The primary concern rises from the burner pitch. If the pitch is reduced, neighbored microflames are eventually combined into one large flame, which leads to dismiss major advantages of microflame (no soot, high-power density). The question raised here is what will be changed by interaction and how it occurs during change of pitch. Answering this question is essential to understand the feature of microflames and to open the way to industirial application.

In this study, we have examined the impact of flame-falme interaction on the behavior of non-premxied microflame in terms of flame shapes, flow flied, and emissions of CH* and H_2O. The examination has been carried out experimentally and numerically by changing the burner pitch.

2 Experimental Setup and Numerical Method

Figure 1 (left) is a schematic drawing of experimental setup. Two straight pipe burners with 0.7 mm ID, 1.0mm OD and 100 mm long are aligned in parallel axis, of which distance is adjusted and

Correspondence to: txh@isc.chubu.ac.jp

measured by a digital length measurement unit (MITUTOYO, SD-15E). From those two burners, methane gas is ejected at the adjusted flowrate by a mass flow controller (HORIBA STEC, SEC-E40). Although burners are fixed in ambient air without forced-flow, co-axial flow is formed at the velocity of 10 to 40 cm/s as previously reported [4, 5], once microflames are established.

In order to observe the behavior of flame interaction, CH* emission image are observed by a 16 bit cooled CCD camera (BITRAN, BS-44UV) through an optical filter with the wavelength of 430 nm (FWHM = 10 nm). In addition, the emission of 945 nm (FWHM = 30 nm) is obtained, which corresponds to H_2O emission in the case of no soot. Those optical filters are mounted on a slide mount which is equipped between the CCD camera and an optical lens (Ai AF Micro Nikkor 105mm F2.8D) .

Numerical model is shown in Fig.1 (right). Circular port burner (outer dia. of d) is placed inside the domain and the prescribed fuel flow rate (corresponding average flow velocity is 0.25 m/s) is imposed at the bottom end to issue the methane into the standard atmosphere (300 K, 101 kPa, air). Since any physicochemical process should be plane symmetry, mirror boundary condition is imposed to the one of side face (see Fig.1) in order to reproduce the interaction of neighbor flame numerically and a distance from burner to the symmetric plane is varied. Other far-field boundaries are set as "open" condition except for the burner inlet as stated above. For simplicity, one-step, finite rate reaction of methane-air system is adopted [6]. Gravity force (negative direction to the jet flow) is taken into account to consider the "upward" buoyancy-driven flow. Combustion module functioned in Front Flow Red (FFR) ver.3.1, which is developed for a parallel multi-scale and multi-physics problems based on SMAC/SIMPLE algorithm under low Mach number approximation [7].

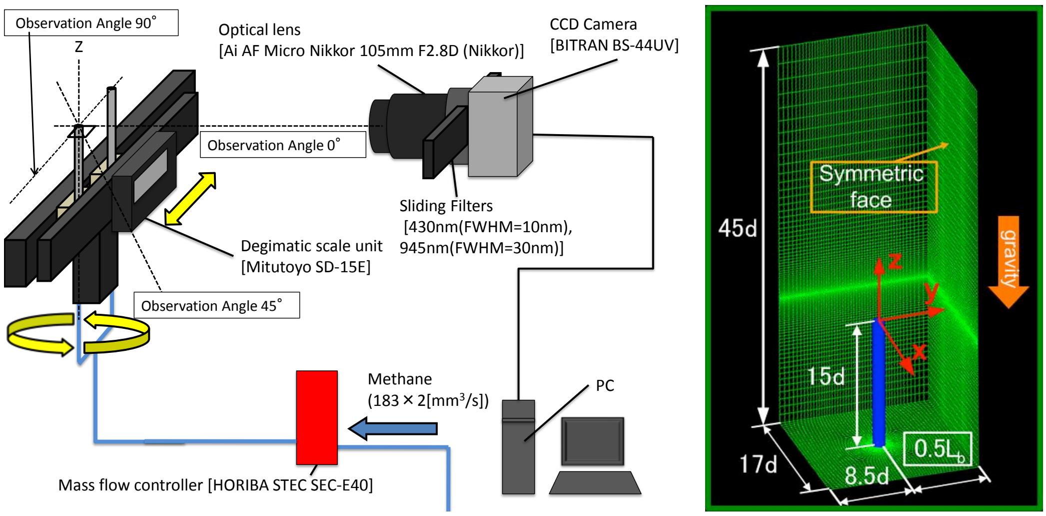

Figure 1. Schematic drawing of experimental apparatus (left) and simulation grids (right).

3 Impact of approach of identical flame to flame shapes

The distributions of reaction zone and hot burned gas obtained from 430 nm and 945 nm images respectively enable us to diagnose the impact of identical flame nearby. Especially for diffusion flame interaction, the distributions of hot burned gas are important because oxygen is supplied from outside of flame, and competing with burned gas. Several typical H_2O and CH^* colormap images of flames overlaid with CH* and H_2O contour are affixed on Fig 2 (a) and 2(b), respectively. We will discuss the data points in Fig. 2 in the following chapter. We do not see any interaction in the images at the distance 8.0 mm. The shape of each microflame is symmetric along burner axis and seemed individual. The diameter of flame is much larger than the one of burner. The flame base locates at about the same height with the burner top. The diameter of flame base is found to be 2.36 mm, which derives that the stand off distance is 0.68 mm. It should be noted that fuel seems to spread rapidly towards the radius just after leaving the exit of the burner, which is similar to the observation of premixed microflame in Ref [8]. This also suggests that some fuel may diffuse to the surroundings without reaching flame zone due to the large diffusion velocity and cause a reduction of combustion efficiency, which will be discussed in the following chapter.

We see flames inclining towards each other at 4.6 mm, as well as a connection of H_2O emission regions from both flames. It should be noted that the H_2O emission region spreads toward each other to attract each other, which suggests some flow interaction. Figure 3 obtained by the numerical simulation shows the increase of axial upward flow between the flames and the incoming radial flow from around two flames. This flow field is considered to be responsible to the connection of H_2O emission regions and flame inclining. Since those are non-premixed flame, lock of oxygen between the flames makes the reaction zone vanished there as shown at 3.6 mm. The CH* intensity is very low between the tops of flames. The flame base exists at 3.6mm but it disappears at 2.8 mm.

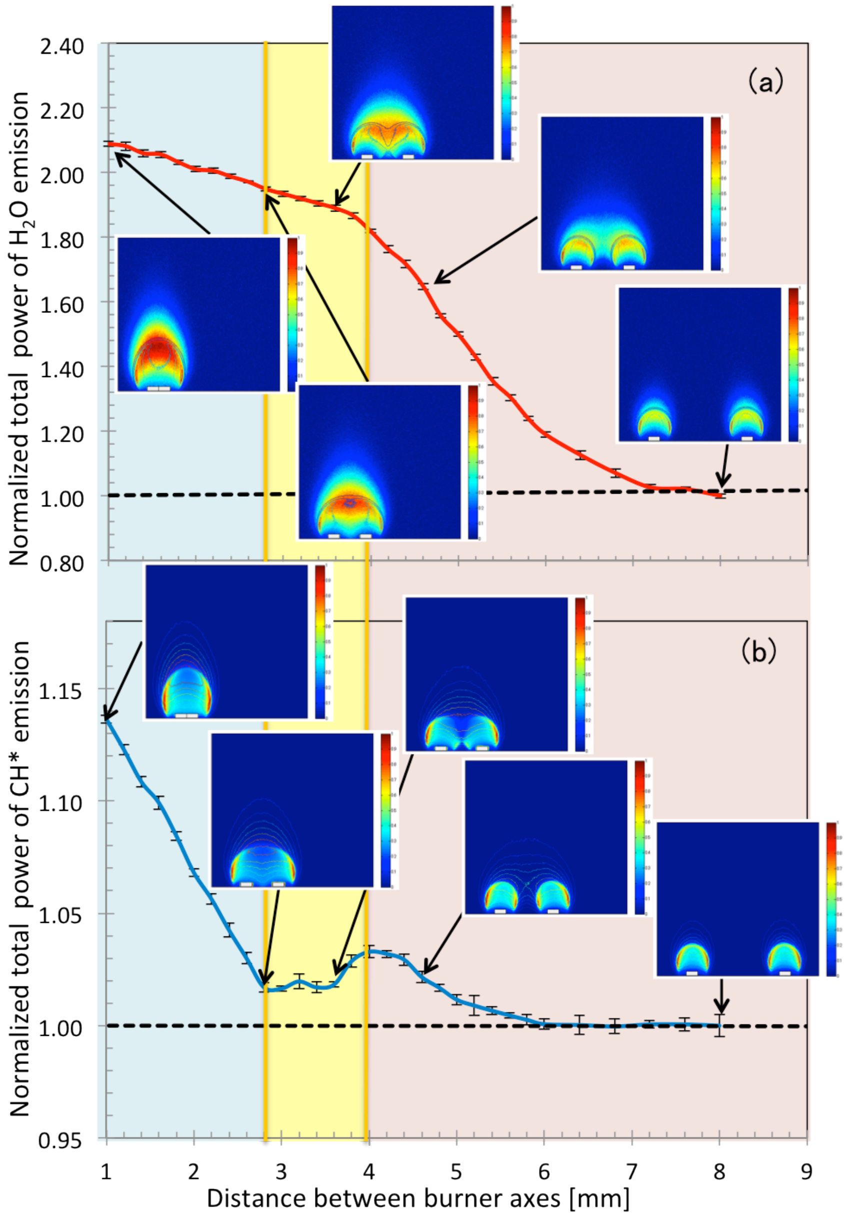

Figure 2. Images of H_2O (a) and CH^* (b) emission at various distance between burner axes and normalized total power of H_2O (a) and CH^* (b) emission.

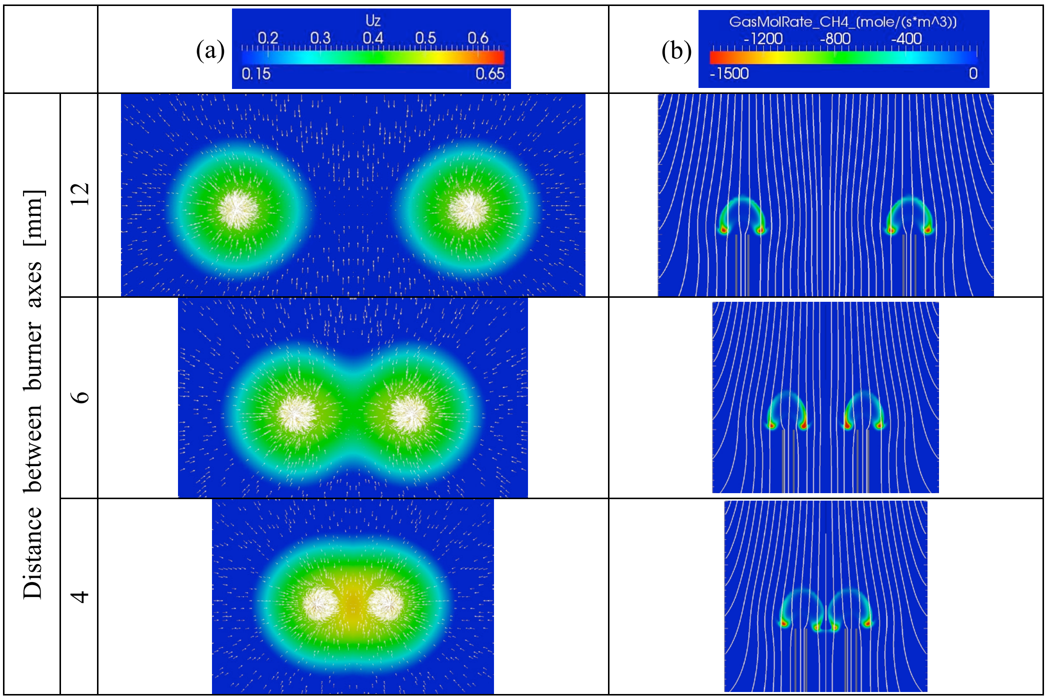

Figure 3 (a) Color map of axial flow velocity Uz at z = 1 mm overlaid with vector map of radial flow velocity. (b) Color map of fuel consumption rate overlaid with streamlines.

4 Change of total power of emission

Simply by integrating the intensity from a CH* image including two whole flames, we can obtain a certain value, that is to be called, a recieved power of emission, P_R. This value depends on total power of emission from flames, P_T, a function of optical pass including effects of distance and absorption, F(s), and factor of optical system, c_o. Thus, the total power of emission from flames can be formulated as $P_R = c_o\mathrm{F}(s)P_T$. Figure 4 shows a schematic drawing to image the concept of received power of emission. From here on, we assume that we do not chnage the factor of optical system. If the layout of flame sheet changes, the function of optical pass will be changed in general. However, in the case of optically thin flames, P_R is independent from the layout of flame sheet, which means F(s) is constant. If F(s) is constant, P_R is directly proportional to P_T. Therefore, total power of emission normalized at a certain condition, in the optically thin case, is derived as $P_T/P_{T0} = P_R/P_{R0}$. Whether the flame is optically thin or not can be verified by whether the recieved power of emission from two flames is constant regardless of the angle of observation. Figure 5 shows the recieved power of emission of CH^* and H_2O from three observation angles at various distance between burner axes. Each data point represents the average of 6 data. The both recieved power of emission do not change by the observation angle through the whole distance between burner axes, which demonstrates that those are optically thin. Therefore, the normalized total power of emission is equal to the normalized *recieved* power of emission.

By the way mentioned above, we obtained the normalized total power of emissions of CH* and H_2O, which is shown in Fig. 2. The error bar indicates a root mean square of scattering data. Based on the trend of total power of emission of CH* and the change of flame shape, interaction can be characterized into three stages. At the first stage, that is, with the distance more than 4 mm, the two flames are separated but warming up each other by working as an adiabatic plane. The flow interaction increases the axial velocity especially at the area between burners as shown in Fig 3(a), which should reduce the fuel leakage out unburned through the stand off distance between the burner exit and flame. Reducing fuel leakage should increase total power of CH* emission as shown in Fig. 2(b).

At the second stage, with the distance from 2.8 to 4.0 mm, the total power of CH* emission decreases as approaching burners. As shown in CH* images at this stage, the flames are gradually getting combined and obviously losing reaction zone between the tops of flames, which should lead to increase fuel leakage.

At the third stage, the distance less than 2.8mm, the total power of CH* emission increases as approaching burners. It should be noted that the flame bases are disappeared at 2.8mm, which means the stand off area is getting reduced from here on. Reducing the stand off area should be one of the reasons to increase the total power of CH* emission. Since no flame base can be seen between burners, practically only one flame exists in this stage. At the early period of this stage, however, the CH* emission at the top of flame is still low, which may still have little fuel leakage from the top. Later on, the CH* emission at the top gradually increase, which should lead to reduce the fuel leakage. This should be another reason to increase the total CH* emission as approaching burners.

The change of the total power of CH* emission is considered to correspond to the change of combustion efficiency as it is explained based on the change of the amount of fuel leakage. It should be noted that the total CH* power of emission of completely combined flame increases in 14 % compared with the individual flames. This also means that combining flame increases combustion efficiency. We discuss the reason of this increase in the following paragraph.

The amount of fuel leakage out unburned through the stand off distance between the burner exit and flame base can be ~20 % as estimated in Ref [1]. From here on, we assume that the fuel loss is 20 % to make a rough estimation. The stand off area is to be reduced by overlapping due to the approach of burner. The estimated reduction of stand off area is 28 % based on the diameter of flame base, 2.36 mm and the outer diameter of burner, 1.0 mm. Based on this, the fuel loss from the contacted burners is estimated as 14.4 %. On the other hand, the experimental results indicate 14 % increase of total power of CH* emission. Based on this, the fuel loss from the contacted burners estimated as 8.8%, which is smaller than the one estimated from the reduction of stand off area. The experimental result of the increase of total power of CH* emission suggests that the combination reduces the fuel loss owing to not only the reduction of stand off area but also some other factors. One of those factors should be the increase of natural convection that increases the upward flow around burners, which opposes to the fuel leakage.

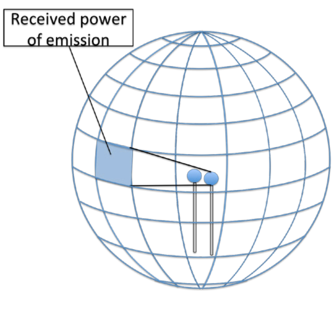

Figure 4. Received power of emission vs. total power of emission.

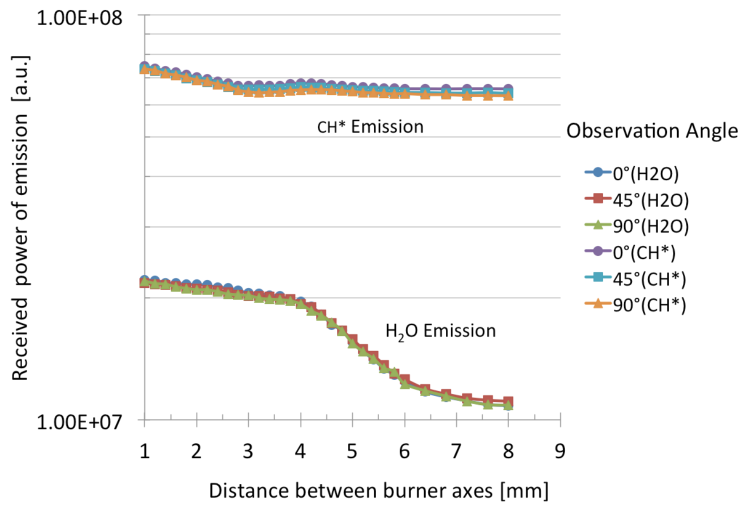

Figure 5. Influence of observation angle in received power of emission.

The total power of H_2O emission can be formulated as

$$\int_{T_0}^{T_1} I_H(T) D_H(T)\, dT \,,$$

where D_H is moles of H_2O at H_2O temperature T, and I_H is power of H_2O emission per unit mole at T. Increase of total power of H_2O emission by approaching burners suggests the increase of amount of high temperature H_2O. Since the change of H_2O production rate is so limited owing to little change of combustion efficiency, the indicated large increase of the total power of H_2O emission is considered mainly due to the shift of H_2O to the high temperature. Therefore, the increase of the total power of H_2O emission is supposed to be reflecting the increase of flame temperature and burned gas, which is consistent with numerical results [5] showing lower flame temperature in the case of microflame.

5 Conclusion

The impact of flame-flame interaction on the behavior of non-premixed microflame has been examined in terms of flame shapes, flow flied, and emissions of CH* and H_2O by changing the burner pitch. The examination has been carried out based on the analysis of emission images observed through optical filter of 430nm and 945 nm, and on the numerical simulation of flow fields by simplest one-step, finite rate reaction of methane-air system in 3-D coordinate system. The normalized total power of emission was obtained from the normalized received power of emission because optically thin assumption was assured by the experimental test.

There are found to be three stages in flame-flame interaction. At the first stage, the two flames are separated but the flow interaction increases the axial velocity between burners and works for the flame to incline toward another flame and slightly increases the total power of CH^*emission. Inclining flame certainly enhances the interaction due to reduction of separation distance. At the second stage, the total power of CH* emission decreases as approaching the burner. The images of CH* at this stage shows that the flames are gradually getting combined and obviously losing reaction zone between the tops of flames. At the third stage, no flame base can be seen between burners, and practically only one flame exists. The total power of CH* emission increases as approaching burners, which seems because of reducing the stand off area and recovering CH* emission at the top of flame.

The change of total power of CH* emission has been well explained by considering the supposed change of fuel leakage and combustion efficiency.

References

[1] Matta LM, Neumeier Y, Lemon B, Zinn BT. (2002). Characteristics of micro scale diffusion flames. Proc. Combust. Inst. 29: 933-939.

[2] Hirasawa T, Nakamura N. (2009). Japanese Unexamined Pat. App. Pub. 2009-007971.

[3] Nakamura N, Hirasawa T. (2010). Kogyo Chosakai Pub. Denshizairyo 7:155-163. (in Japanese).

[4] Nakamura Y, K. Saito, Nagare 20 (2001) 74-82. (in Japanese)

[5] Nakamura Y, Yamashita H, Saito K. (2006). A numerical study on extinction behaviour of laminar micro-diffusion flames. Combust. Theory Modeling 10 (6): 927-938.

[6] Westbrook CK. (1981). Simplified Reaction Mechanism for the Oxidation of Hydrocarbon Fuels in Flames. Combust. Sci. Tech.27:31-43.

[7] http://www.ciss.iis.u-tokyo.ac.jp/rss21/theme/multi/fluid/fluid_softwareinfo.html

[8] Yuasa S, Oshimi M, Nose H, Tennichi Y. (2005). Concept and combustion characteristics of ultra-micro combustors with premixed flame. Proc. Combust. Inst. 30:2455-2462.